

## Vacancies and voids in hydrogenated amorphous silicon

A. H. M. Smets,<sup>a)</sup> W. M. M. Kessels, and M. C. M. van de Sanden

Center of Plasma Physics and Radiation Technology, Department of Applied Physics, Eindhoven University of Technology, P.O. Box 513, 5600 MB Eindhoven, The Netherlands

(Received 14 November 2002; accepted 16 January 2003)

The hydride configurations in the hydrogenated amorphous silicon (*a*-Si:H) network have been studied by means of infrared absorption spectroscopy. The results on the film mass density of *a*-Si:H deposited by means of an expanding thermal plasma reveal the presence of two distinct regions in terms of hydrogen content and microstructure: below approximately 14 at. % H *a*-Si:H contains predominantly divacancies decorated by hydrogen, above 14 at. % H *a*-Si:H contains microscopic voids. These two distinct regions provide additional information on the origin of the low and high hydride stretching modes at 1980–2010 and 2070–2100  $\text{cm}^{-1}$ , respectively. © 2003 American Institute of Physics. [DOI: 10.1063/1.1559657]

Hydrogen plays a crucial role in many properties of hydrogenated amorphous silicon (*a*-Si:H), such as in lowering the *a*-Si:H defect densities to  $10^{15}$ – $10^{16}$   $\text{cm}^{-3}$ ,<sup>1</sup> in controlling the optoelectronic properties and possibly in the Staebler–Wronski effect (SWE).<sup>2</sup> Therefore, various studies have been devoted to the question how hydrogen exactly resides in the *a*-Si:H network<sup>3–6</sup> and many different configurations have been observed and suggested. Several studies have revealed that the predominant bonding environment for hydrogen is a cluster of four to seven atoms and divacancies have been proposed as a possible configuration to build in these clusters in the *a*-Si:H network.<sup>3–6</sup> The vacancy is defined as a lattice site at which up to 3 Si atoms are missing (see Fig. 1)<sup>4,7</sup> and recently it was postulated that the vacancies can possibly act as the precursor for the light induced dangling bond creation by the SWE.<sup>7</sup> On the other hand, nuclear magnetic resonance (NMR) studies in combination with infrared (IR) absorption studies suggested that 4 at. % H of bonded hydrogen is in an isolated phase, i.e., a monohydride without any hydrogen as nearest neighbor.<sup>3,6,8</sup> Furthermore, not all hydrogen is atomically bonded to a Si atom, but up to 40% could be present in the form of isolated hydrogen molecules in the *a*-Si:H network.<sup>9</sup> Small angle x-ray scattering studies<sup>10</sup> revealed that even larger features than vacancies, i.e., “microscopic” voids of 2 up to 4 nm, are present in the *a*-Si:H network as well. The aim of this letter is to get additional insight into how hydrogen resides into the *a*-Si:H network and especially how the presence of the vacancy and void configurations depend on the hydrogen content. Information on the *a*-Si:H microstructure is obtained using the relation between the *a*-Si:H film mass density and the intensity of the hydride absorption modes in the IR.

Over 50 *a*-Si:H films, with a hydrogen content  $c_H$  ranging from 2 at. % H up to 26 at. % H, have been deposited on *c*-Si substrates by means of the expanding thermal plasma (ETP). A broad plasma parameter window, i.e., the growth rate  $R_d$  ranges from 2 to 120  $\text{\AA}/\text{s}$  and the substrate temperature ranges from 100 to 500  $^\circ\text{C}$ , have been used. The refractive index  $n$ , thickness, mode absorptions, hydrogen content

$c_H$  and mass density  $\rho_{a\text{-Si:H}}$  of the *a*-Si:H films are obtained from Fourier-transform IR measurements in transmission using a Bruker Vector 22 Fourier transform spectroscope ( $\omega = 340$  up to  $7500$   $\text{cm}^{-1}$ ). The refractive index and the film thickness are determined from the interference fringes of the resulting background spectrum in the nonabsorbing spectrum range, as described elsewhere.<sup>11</sup> The Si–H<sub>*x*</sub> hydride vibrations have three characteristic absorptions in *a*-Si:H IR spectrum: wagging modes at  $640$   $\text{cm}^{-1}$ , a bending scissor mode at  $840$ – $890$   $\text{cm}^{-1}$ , and two stretching modes at  $1980$ – $2030$  and  $2060$ – $2160$   $\text{cm}^{-1}$ , in this letter referred to as the low stretching mode (LSM) and the high stretching mode (HSM), respectively. The density  $N_x$  of a Si–H<sub>*x*</sub> mode is proportional to the integrated absorption strength of the given mode:  $N_x = A_x \int \omega^{-1} \alpha(\omega) d\omega$  with  $\alpha(\omega)$  as the absorption coefficient and  $A_x$  as the proportional constant. Every H bonded to silicon contributes to the  $640$   $\text{cm}^{-1}$  wagging mode and consequently this mode is used to determine the hydrogen density. For ETP *a*-Si:H films  $A_{640} = 1.6 \times 10^{19}$   $\text{cm}^{-2}$ , calibrated by means of elastic recoil detection analysis.<sup>12</sup> The interpretation of the LSM and HSM modes is more complex, which is clear from the extensive discussions in the literature on the origin of the LSM and HSM. The LSM is assigned to only monohydrides.<sup>5,6,11,13,14</sup> However, the question of which monohydride configurations contribute to the LSM is still under discussion.<sup>5,6</sup> A similar discussion exists for the HSM mode: in Ref. 13 the HSM is assigned to a stretching mode of only dihydrides, whereas others also assign the HSM as

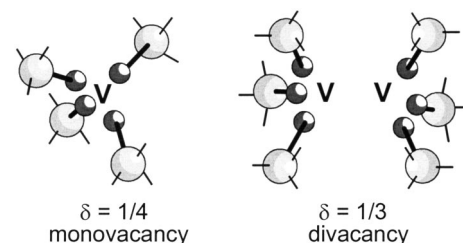


FIG. 1. The three-dimensional representation of the short-range order of a monovacancy and divacancy, having a hydrogen incorporation parameter of  $\delta = 1/4$  and  $\delta = 1/3$ , respectively. The “missing” silicons are represented by V.

<sup>a)</sup>Electronic mail: a.h.m.smets@tue.nl

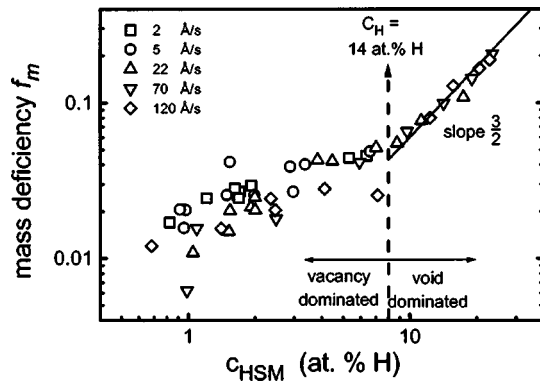


FIG. 2. The mass deficiency  $f_m$  vs HSM mode hydrogen content  $c_{\text{HSM}}$ . The slope of the solid line at  $c_{\text{HSM}} > 8$  at. % H is  $3/2$ , corresponding to a void dominated  $f_m$ . At  $c_{\text{HSM}} = 8$  at. % H the total hydrogen content  $c_{\text{H}} = 14$  at. % H [see Fig. 3(b)] is indicated by the dashed line.

monohydrides group incorporated at internal void surfaces.<sup>5</sup> By comparison of the ratios of the modes we have determined that  $A_{\text{LSM}} \approx A_{\text{HSM}} = 9.1 \times 10^{19} \text{ cm}^{-2}$  using a procedure similar to that applied in Refs. 5 and 6. This proportionality constant will be used throughout this letter.

The mass density of the films is determined by means of the Clausius–Mossotti equation, which describes the refractive index  $n$  in terms of Si–Si and Si–H bond harmonic dipole oscillators.<sup>4</sup> For  $a$ -Si:H films with 100% amorphous fraction the mass density  $\rho_{a\text{-Si:H}}$  can be described as<sup>4</sup>

$$\rho_{a\text{-Si:H}} = \left( \frac{n^2 - 1}{n^2 + 2} \right) \frac{3m_{\text{Si}}}{4\pi \left[ 2\alpha_{\text{Si-Si}} + \frac{c_{\text{H}}}{1 - c_{\text{H}}} \left( \alpha_{\text{Si-H}} - \frac{1}{2} \alpha_{\text{Si-Si}} \right) \right]}, \quad (1)$$

where  $m_{\text{Si}}$  is the mass of the Si atom,  $\alpha_{\text{Si-Si}}$  and  $\alpha_{\text{Si-H}}$  are the bond polarizability in the amorphous phase of the Si–Si and Si–H bond, respectively. The value  $\alpha_{\text{Si-Si}} = 1.96 \times 10^{-24} \text{ cm}^3$  and  $\alpha_{\text{Si-H}} = 1.36 \times 10^{-24} \text{ cm}^3$  are taken from Ref. 4.

The measured mass deficiency  $f_m$ , defined as  $f_m = (1 - \rho_{a\text{-Si:H}}/\rho_{a\text{-Si}})$  with  $\rho_{a\text{-Si}} = 2.29 \text{ g cm}^{-3}$  the density of  $a$ -Si,<sup>4</sup> is plotted versus the hydrogen content contributing to the HSM  $c_{\text{HSM}}$  in Fig. 2. Note, that the total hydrogen content  $c_{\text{H}} = c_{\text{LSM}} + c_{\text{HSM}}$  and the total hydrogen content  $c_{\text{H}}$  of  $14 \pm 2$  at. % H, corresponding to HSM hydrogen content  $c_{\text{HSM}}$  of 8 at. % H [see Fig. 3(b)], is indicated by a dashed line in Fig. 2. Two regions can be distinguished: for  $c_{\text{HSM}} > 8$  at. % H ( $c_{\text{H}} > 14 \pm 2$  at. % H)  $f_m$  varies as  $(c_{\text{HSM}})^{3/2}$  whereas for  $c_{\text{HSM}} < 8$  at. % H ( $c_{\text{H}} < 14 \pm 2$  at. % H)  $f_m$  differs evidently from the  $(c_{\text{HSM}})^{3/2}$  dependence. As has been proposed by others in Refs. 5 and 6, the HSM corresponds to hydrogen bonded to a void surface. Since microscopic voids with a radius of 1 up to 4 nm correspond to many missing Si atoms (200 up to  $\sim 10^4$ , respectively),<sup>10</sup> they should have a direct impact on the film density. Within this picture we can easily explain the observed dependence: if we assume that  $c_{\text{HSM}}$  indeed corresponds to hydrogen at void surfaces than  $c_{\text{HSM}}$  is directly related to the averaged internal void surface  $S_{\text{void}}$ . The averaged void volume  $V_{\text{void}}$  scales linear with the mass deficiency  $f_m \sim V_{\text{void}} \sim (S_{\text{void}})^{3/2} \sim (c_{\text{HSM}})^{3/2}$ . The observed

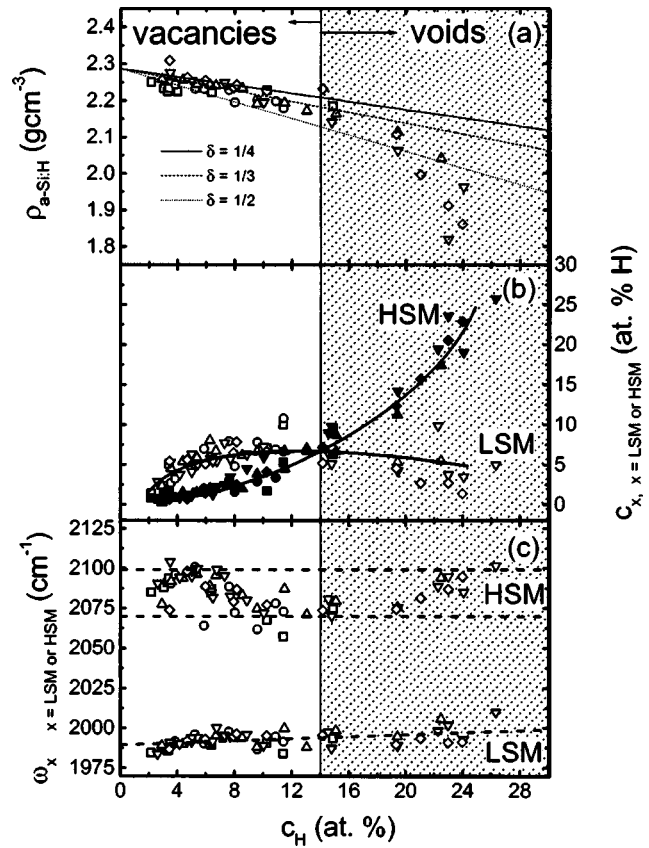


FIG. 3. (a) The mass film density  $\rho_{a\text{-Si:H}}$  vs the hydrogen content. The lines correspond to the mass film density dependence ruled by monovacancy  $\delta = 1/4$  (solid line), divacancy  $\delta = 1/3$  (dashed line), and the  $m$ -vacancy limit  $\delta = 1/2$  (dotted line) following Eq. (2). (b) The stretching mode hydrogen contents  $c_{\text{LSM}}$  and  $c_{\text{HSM}}$  plotted vs the hydrogen content. (c) The obtained eigen frequency positions  $\omega_{\text{LSM}}$  and  $\omega_{\text{HSM}}$  vs the hydrogen content.

$f_m \sim (c_{\text{HSM}})^{3/2}$  dependence therefore confirms that for  $c_{\text{HSM}} > 8$  at. % H ( $c_{\text{H}} > 14 \pm 2$  at. % H) the film density is determined by the voids. Furthermore, the dependence proves that hydrogen bonded at void surfaces dominates the HSM absorption. As a consequence the  $f_m$  behavior on  $c_{\text{HSM}}$  for  $c_{\text{HSM}} < 8$  at. % H ( $c_{\text{H}} < 14 \pm 2$  at. % H) is not or not only ruled by voids.

More information about the  $c_{\text{H}} < 14 \pm 2$  at. % H region can be obtained if the film density is plotted versus the  $c_{\text{H}}$  [see Fig. 3(a)]. This dependence can be used as a tool to study whether the hydrides are clustered, as also demonstrated in Ref. 4. If we assume that the film density  $\rho_{a\text{-Si:H}}$  depends on the  $a$ -Si atom volume density  $\rho_{a\text{-Si}}$  and the hydrogen volume density  $\rho_{\text{H}}$ , the following relation should hold<sup>4</sup>

$$\rho_{a\text{-Si:H}} = \rho_{a\text{-Si}} - (\delta \rho_{a\text{-Si}} - \rho_{\text{H}}) c_{\text{H}}, \quad (2)$$

where  $\delta$  is the hydrogen incorporation parameter, which depends upon the configuration in which hydrogen is incorporated. Remes *et al.*<sup>4</sup> proposed a model in which a monovacancy is a configuration which corresponds to  $\delta = 1/4$ , a divacancy to  $\delta = 1/3$  (see both in Fig. 1), and a small polymer like  $m$  vacancy to  $\delta = m/(2m + 2) < 1/2$ . The film density for a given vacancy type following from Eq. (2) are also plotted in Fig. 3(a). The data in Fig. 3(a) suggest that for 4 at. % H  $< c_{\text{H}} < 14 \pm 2$  at. % H the hydrogen incorporation is best described by  $\delta = 0.33 \pm 0.03$ , corresponding to roughly a diva-

cancy dominated film density. This result is in agreement with reported NMR measurements,<sup>3</sup> and results by Remes *et al.*<sup>4</sup> For  $c_H > 14 \pm 2$  at. % H the film density cannot be described by a vacancy model, as the data drop below the theoretical  $\delta = 1/2$  line, as we also concluded from Fig. 2. The dependence of  $\rho_{a\text{-Si:H}}$  on  $c_H$  and  $c_{\text{HSM}}$  [Figs. 2 and 3(a)] reveal that for  $c_H < 14 \pm 2$  at. % H roughly the divacancies and for  $c_H > 14 \pm 2$  at. % H the microscopic voids determine the film density. Note, that the value of 14 at. % H accounts for *a*-Si:H deposited by means of the ETP technique and this value could differ for *a*-Si:H films deposited by other techniques. Furthermore, Fig. 2 shows that only *a*-Si:H films deposited at high rates ( $R_d > 5 \text{ \AA/s}$ ) and low substrate temperatures ( $T_{\text{sub}} < 250 \text{ }^\circ\text{C}$ ) are in the region where voids determine the density. The incorporation mechanism of voids and its relation to the growth rate and substrate temperature will be discussed elsewhere.

The observation that the microstructure depends on the total hydrogen incorporated and that two regions can be distinguished can help in the understanding of the origin of the LSM and HSM. In Fig. 3(b) the LSM and HSM content as a function of the total hydrogen content is plotted. For  $c_H < 14 \pm 2$  at. % H the LSM dominates. Since in this range the hydrogen is preferentially bonded at divacancies [see Fig. 3(a)], mainly monohydrides in a divacancy configuration contribute to the LSM. Moreover, the results in Figs. 3(a) and 3(b) rule out isolated monohydrides, having a  $\delta$  around 1, as an important contributor to the LSM for  $c_H < 14 \pm 2$  at. % H. Additional arguments for a compact hydrogen incorporation in vacancies can be gained from the LSM eigenfrequency  $\omega_{\text{LSM}}$ . The eigenfrequency  $\omega_{\text{LSM}}$ , as shown in Fig. 3(c), is positioned between 1980 and 2010  $\text{cm}^{-1}$ , which is a shift of  $\Delta\omega \sim 100 \text{ cm}^{-1}$  from the  $\text{Si}_3\text{-SiH}$  monohydride stretching mode within polysilane molecules at 2099  $\text{cm}^{-1}$ .<sup>15</sup> Cardona<sup>15</sup> deduced that the shift scales like  $\Delta\omega \sim R^{-3}$  as a result of the depolarizing field produced by the vibrating Si-H inside a small cavity with radius  $R$ . The mono- and divacancies are the most compact configurations to incorporate monohydrides (see Fig. 1). Consequently, these monohydride configurations with smallest  $R$ , should have the largest shift and therefore should be the first candidates to contribute to the LSM in line with our results.

For  $c_H > 14 \pm 2$  at. % H the HSM absorption dominates the LSM absorption, corresponding to  $\text{SiH}_x$  on the void surfaces. In the vacancy dominated region, i.e.,  $\delta = 1/3$ , still a HSM absorption is measured, which not necessarily corresponds to hydrogen at a void surface (see Fig. 2). Instead it could also correspond to a dihydride which is not bonded at an internal surface. The only compact way to incorporate a dihydride, such that  $\delta < 1/2$  is satisfied, is the configuration in which the dihydride is part of two monovacancies.<sup>7</sup> This compact dihydride configuration requires at least six mono-

hydrides, or in other words  $c_{\text{LSM}}/c_{\text{HSM}} \geq 3$ , and therefore according to Fig. 3(b) if this configuration exists, it can only be an important contributor to the LSM for  $c_H < 6$  at. % H. As a consequence the HSM is directly linked with hydrogen bonded to void surfaces for  $c_{\text{HSM}} > 2$  at. %. The HSM eigenfrequency  $\omega_{\text{HSM}}$  values [Fig. 3(c)] vary between 2070 and 2100  $\text{cm}^{-1}$  and the full width at half maximum of the HSM is 70  $\text{cm}^{-1}$ . Since these void surfaces can be interpreted as “normal” passivated Si:H surfaces we can compare them with the known surface hydride eigenfrequencies. The observed frequencies of monohydrides on a silicon surface range from 2072 up to 2099  $\text{cm}^{-1}$  whereas the dihydride vibration varies from 2097 up to 2119  $\text{cm}^{-1}$ . Therefore, the observed  $\omega_{\text{HSM}}$  range suggests that both mono- and dihydrides contribute to the HSM, while the monohydrides have the largest contribution to the HSM.

In summary, the IR absorption spectroscopy on *a*-Si:H films deposited by ETP reveals that the film density has two distinct regions in terms of hydrogen configurations and microstructure: (1) one region is determined on the average by divacancies ( $c_H < 14 \pm 2$  at. %) and one region is determined by macroscopic voids ( $c_H > 14 \pm 2$  at. %). The monohydrides in vacancies contribute dominantly to the LSM, whereas hydrides on a void surface contribute significantly to the HSM.

The authors acknowledge support of this research by NOVEM and TDO.

- <sup>1</sup>J. Lewis, G. A. N. Connell, W. Paul, J. R. Pawlik, and R. J. Temkin, in *Tetrahedrally Bonded Amorphous Semiconductors*, edited by M. H. Brodsky and S. Kirkpatrick (American Institute of Physics, New York, 1974).
- <sup>2</sup>D. L. Staebler and C. R. Wronski, *Appl. Phys. Lett.* **31**, 292 (1977).
- <sup>3</sup>J. Baum, K. K. Gleason, A. Pines, A. N. Garroway, and J. A. Reimer, *Phys. Rev. Lett.* **56**, 1377 (1986).
- <sup>4</sup>Z. Remes, M. Vanecek, A. H. Mahan, and R. S. Crandall, *Phys. Rev. B* **56**, 12710 (1997), and references therein.
- <sup>5</sup>W. Beyer and M. S. Abo Ghazala, *Mater. Res. Soc. Symp. Proc.* **507**, 601 (1998).
- <sup>6</sup>J. Daey Ouwens and R. E. I. Schropp, *Phys. Rev. B* **54**, 17759 (1996).
- <sup>7</sup>S. B. Zhang and H. M. Branz, *Phys. Rev. Lett.* **87**, 105503 (2001).
- <sup>8</sup>W. E. Carlos and P. C. Taylor, *Phys. Rev. B* **26**, 3605 (1982).
- <sup>9</sup>R. E. Norberg, D. J. Leopold, and P. A. Fedders, *J. Non-Cryst. Solids* **227-230**, 124 (1998).
- <sup>10</sup>A. H. Mahan, Y. Xu, D. L. Williamson, W. Beyer, J. D. Perkins, M. Vanecek, L. M. Gedvillas, and B. P. Nelson, *J. Appl. Phys.* **90**, 5038 (2001).
- <sup>11</sup>R. J. Severens, G. J. H. Brussaard, M. C. M. van de Sanden, and D. C. Schram, *Appl. Phys. Lett.* **67**, 491 (1995).
- <sup>12</sup>W. M. M. Kessels, M. C. M. van de Sanden, R. J. Severens, L. J. van IJzendoorn, and D. C. Schram, *Mater. Res. Soc. Symp. Proc.* **507**, 529 (1998).
- <sup>13</sup>G. Lucovsky, R. J. Nemanich, and J. C. Knights, *Phys. Rev. B* **19**, 2064 (1979).
- <sup>14</sup>A. A. Langford, M. L. Fleet, B. P. Nelson, W. A. Lanford, and N. Maley, *Phys. Rev. B* **45**, 13367 (1992).
- <sup>15</sup>M. Cardona, *Phys. Status Solidi A* **118**, 463 (1983).